

Lattice Boltzmann Simulation of Fluid Flow and Heat Transfer Through Porous Media – A Pore-Scale Approach

Annunziata D’Orazio^a, Arash Karimipour^b, Iman Moradi^{a*}

^aDipartimento di Ingegneria Astronautica, Elettrica ed Energetica, Sapienza University of Rome, Italy

^bDepartment of Mechanical Engineering, Najafabad Branch, Islamic Azad University, Najafabad, Iran
Annunziata.dorazio@uniroma1.it, Arashkarimipour@gmail.com, Iman.moradi@uniroma1.it

Abstract: The size and arrangement of the obstacles that form in the porous media have an influence on fluid flow and heat transfer., even in the same porosity. To address this issue, the present study simulated three obstacles in both regular and different staggered arrangements through a channel to compare the effect of staggered and regular arrangements, as well as different obstacle positions in the same porosity, on fluid flow and heat transfer. In the present study, the Single Relaxation Time Lattice Boltzmann Method, with Bhatnagar-Gross-Krook (BGK) approximation and D2Q9 model, is implemented for the numerical simulation. The temperature field is modeled using a Double Distribution Function (DDF) approach. Results are presented in terms of velocity and temperature fields, streamlines, percentage of pressure drop and Nusselt number of the obstacles walls. Also, the correlation between tortuosity and Nusselt number of the walls of the obstacles, has been proposed. The results show that by changing the arrangement of the obstacles from regular to staggered, with the same porosity, the Nusselt number of the obstacles increased by up 167%.

Keywords: Lattice Boltzmann method; Heat transfer; Porous media; Pore-Scale; Porosity; tortuosity

1- Introduction

In recent decades, the use of porous media has increased greatly due to their high contact area per volume. On the other hand, the Lattice Boltzmann method is a suitable approach for the simulation of heat and mass transfer through porous media and it shows great capabilities in many applications [1–2], such as electronic devices and thermal engineering [3–6], chemical engineering [7–10], materials science [11–14], oceanography [15], geophysics [16] and medicine [17].

There are two main methods for simulating porous media, namely the pore-scale (PS) and the representative elementary volume (REV) methods. In the REV method, the fluid flow and heat transfer through the porous media is simulated by adding some terms to the LBM equation related to the porous media properties such as porosity and permeability. The disadvantage of this method is that the effect of porous media structure on fluid flow and heat transfer is not as visible as it should be. To investigate the effect of porous media structure and the effect of solid obstacles on the fluid flow and heat transfer, the pore-scale method is proposed. In this case, the flow behavior through the solid parts of porous media can be investigated. To gain a better understanding of this issue, some recent studies have been reviewed in the following.

I. Moradi and A. D’Orazio [1] have done a pore scale porous media by using LBM. They studied sixteen different obstacle arrangements and three different sizes of obstacles as a pore

scale porous media in a constant porosity. The simulation includes a heated wall channel and cold porous obstacles. The results have shown that increasing the number of obstacles for the same porosity, the Nusselt number and the tortuosity also increase. Hu Wang et al. [18] studied thermal resistance and pumping power issues with the aim of optimizing a double-layer microchannel heat sink with semi-porous fins by using a multi-objective genetic algorithm, achieving better performance by using a porous media geometry.

In [19], fluid flow and heat transfer through metal foams as porous media have been studied using LBM and MRT method and BGK approximation. In [20, 21], convection heat transfer in porous media is simulated by LBM with the aim of application in solar collectors, geothermal systems, and life sciences. An investigation of flow and conjugate heat transfer in an open-cell metal foam with high porosity as a pore-scale model has been carried out by [22]. In this study, five (REV) samples with different values of porosity, 0.80, 0.85 and 0.90 and variety of pore density, 10, 20 and 30 PPI are modelled. A decoupled lattice Boltzmann solver is developed in these numerical simulations by using multi-relaxation time (MRT) for flow and regularized lattice Boltzmann (RLB) method for advection-diffusion. The solver in this research, has simulated advection-diffusion in the non-Darcy regime.

Chen et al. [23] by coupling the lattice Boltzmann method and discrete element method (DEM) provided a numerical

framework to simulate a self-compacting concrete (SCC) flows, through a rock-filled concrete RFC as a porous medium. The results show that the SCC flow in multichannel porous media is self-adjusting and willing to pass through larger gaps. A. D’Orazio and A. Karimipour [24] developed the lattice Boltzmann method performance to simulate the constant heat flux boundary condition along the microchannel walls with slip velocity and buoyancy forces for the first time. X Huang et al. [25] studied the influence of diffusion coefficients in porous fibrous material and made a comparison between the results of Lattice Boltzmann method (LBM) and the Pore Network Modeling (PNM) in this pore-scale structure simulation.

M. Zhang et al. [26] simulated a two-dimensional steady state fluid flow and heat transfer in a porous medium at constant temperature using LBM. The simulation focused on around and through the porous objects. In [27], the numerical simulation for convection heat transfer through porous media under local thermal non-equilibrium (LTNE) condition was carried out by the LBM.

As mentioned above, the influence of the use of porous media in heat and mass transfer applications has increased greatly in the recent decades. Nevertheless, there is a need for results that explain the relationship between porous media properties

and heat transfer in more detail. In the present study, the fluid flow and heat transfer through the pore scale porous media are simulated by using LBM with the pore scale approach. The effect of the arrangement of the obstacles on the fluid flow and heat transfer is studied for the same porosity. Finally, the correlation between the tortuosity and the Nusselt number of the walls of the obstacles is proposed, to facilitate the identification of the size and arrangement of obstacles in the porous media in heat transfer applications.

2- Model Description

As it can be seen in the figure 2., there is a porous region, represented by a pore-scale approach, in the middle of a channel with insulated walls. The porous medium contains the square obstacles in five different arrangements, such as in-line, staggered, symmetrical and non-symmetrical. Water is the working fluid entering to the channel with $Re=10$ and $\theta=0$, which are the Reynolds number and nondimensional temperature, respectively. The obstacles are hot and $\theta=1$. In the present study, the porosity is 75% ($\epsilon=75%$) in all the simulations and the arrangements are numbered from 1 to 5 as shown in the figure below.

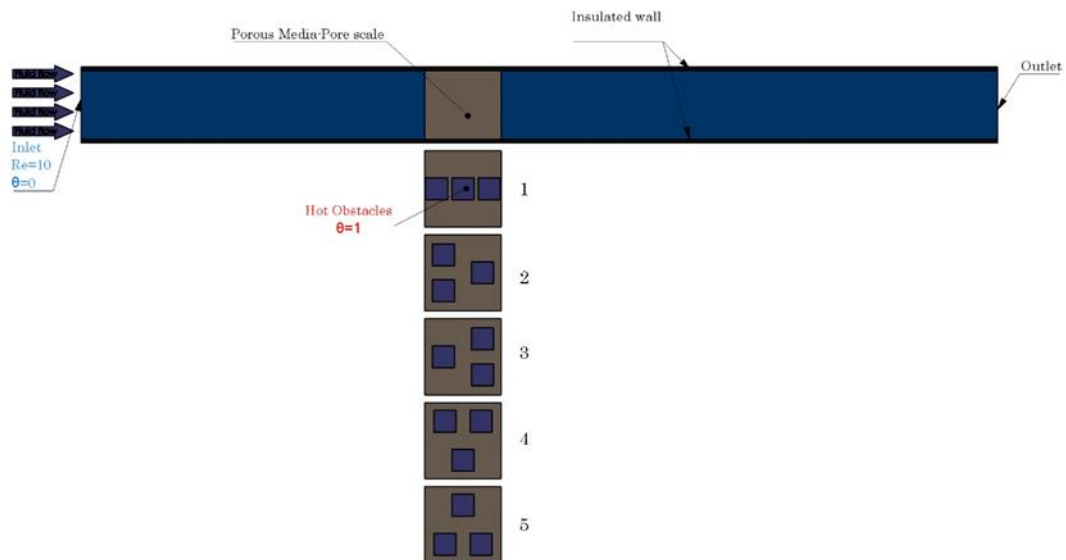


Fig. 1. Different arrangement of porous obstacles through the channel

3-Governing Equation

The Lattice Boltzmann Method is chosen to simulate the flow by using the discretized Boltzmann equation. The Bhatnagar-Gross-Krook (BGK) model [28] is implemented. In this

method, the motion of the fluid particles is restricted to specific i -directions with specific microscopic velocities c_i . The D2Q9 model is useful for the advection-diffusion problems; the specified i -directions of this model are shown in Fig. . The density distribution function can be written as:

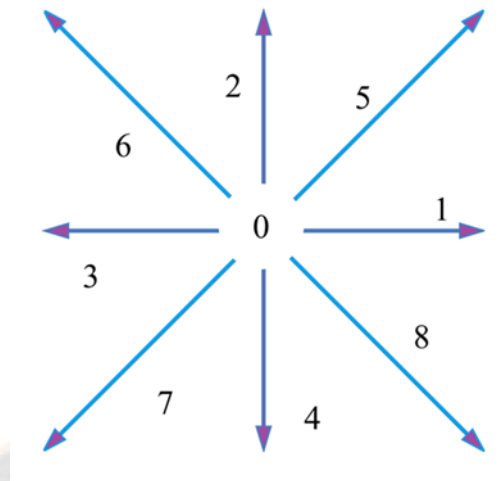


Fig. 2. Schematic diagram of the lattice D2Q9 model

$$f_i(x + c_i \Delta t, t + \Delta t) - f_i(x, t) = \Omega_i(f) \quad (1)$$

where the discrete distribution function is represented by f_i and the discrete velocity by c_i . In addition, Ω_i is the discrete collision operator. The collision operator of the Single Relaxation Time model is proposed as follows:

$$\Omega_i(f) = \frac{1}{\tau} (f_i^{eq} - f_i) \quad (2)$$

where τ is the relaxation time and f_i^{eq} is the equilibrium distribution function.

Regarding the (1) and (2), a SRT-LBM discrete distribution function by using BGK approximation is as (3). where $f_i^{eq}(x, t)$ is the equilibrium distribution function, shown in (4),

$$\begin{aligned} f_i(x + c_i \Delta t, t + \Delta t) \\ = f_i(x, t) + \frac{1}{\tau_f} (f_i^{eq}(x, t) \\ - f_i(x, t)) \end{aligned} \quad (3)$$

$$f_i^{eq}(x, t) = w_i \rho \left[1 + \frac{c_i \cdot u}{C_s^2} + \frac{(c_i \cdot u)^2}{2C_s^2} - \frac{u^2}{2C_s^2} \right] \quad (4)$$

In (4), w_i is the weighting coefficient, and C_s is the lattice sound speed. The relationship between kinematic viscosity and relaxation time is given by equation (5). Also, according to the discrete distribution function f_i , the macroscopic variables, such as density and velocity, have been written as equations (6) and (7)

$$\vartheta = \Delta t C_s^2 (\tau_f - \frac{1}{2}) \quad (5)$$

$$\rho = \sum_0^8 f_i \quad (6)$$

$$u = \frac{1}{\rho} \sum_0^8 f_i c_i \quad (7)$$

Similar equations for the temperature field are given below:

$$g_i(x + c_i \Delta t, t + \Delta t) \quad (8)$$

$$= g_i(x, t) + \frac{1}{\tau_g} (g_i^{eq}(x, t) - g_i(x, t))$$

$$\alpha = \Delta t C_s^2 (\tau_g - \frac{1}{2}) \quad (9)$$

$$g_i^{eq}(x, t) = \omega_i \theta \left[1 + \frac{c_i \cdot u}{C_s^2} \right] \quad (10)$$

$$T = \sum_0^8 g_i \quad (11)$$

where τ_g is the relaxation time for the temperature distribution function, which calculated form (9), g_i^{eq} is the temperature equilibrium distribution function, computed by (10), and T is the macroscopic temperature.

4-Results and discussion

The distribution of the dimensionless temperature θ through the channel with three obstacles as a solid part of the porous media is shown in Fig. 3. As can be seen, the obstacles are hot ($\theta=1$) and the water at the inlet is cold ($\theta=0$). In addition, the upper and lower walls of the channel are insulated. This figure shows that the minimum temperature at the outlet belongs to arrangement 1, with a value of $\theta=0.5$

approximately, and the maximum belongs to arrangements 2 and 3, with a value of $\theta=0.75$ approximately. Arrangements 4 and 5, which are not symmetrical in the X direction, approached uniform temperature distribution after a long

distance from the obstacles. Arrangement 2 and 3, which are symmetrical in X direction, approached the uniform temperature distribution after a short distance from the obstacles.

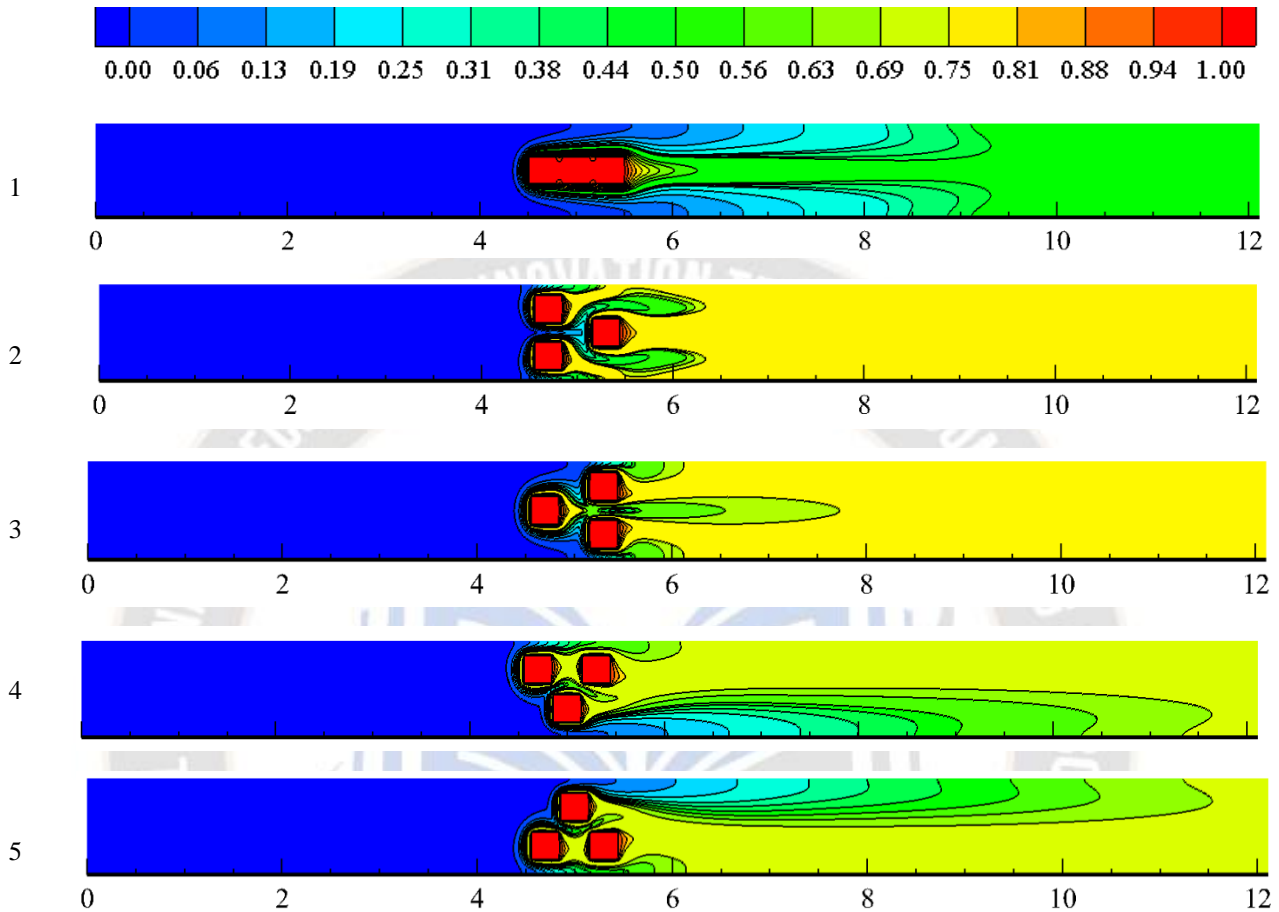


Fig. 3. Non-dimensional distribution of temperature θ through the channel for different obstacles arrangements (1 to 5)

The Nusselt Number of the obstacles in different arrangements from 1 to 5 is shown in Fig. 4. The local and average Nusselt number of the walls of obstacles are calculated from equations 12 and 13.

$$Nu_x = \frac{hD_h}{k} = D_h \frac{\partial\theta/\partial y}{T_w - T_m} \quad (12)$$

$$Nu_{x,avg} = \frac{1}{L} \int_0^L Nu_x dx \quad (13)$$

As can be seen in Fig. 4, the Nusselt number of the obstacle wall, increased sharply by up to 167% by changing the arrangement from in-line to staggered. In addition, by changing the position of the obstacles in the staggered arrangement, the Nusselt number of the obstacles wall also changed. Consequently, for the same porosity and constant number of solid obstacles in a porous medium, the heat transfer could be increased by up to 167% by changing the arrangement of the obstacles.

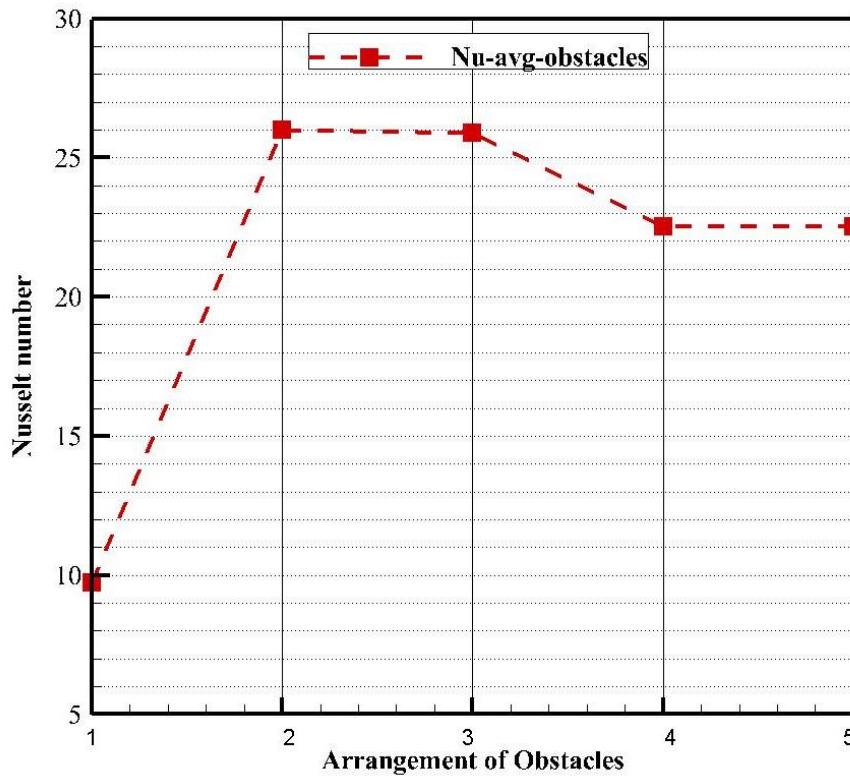


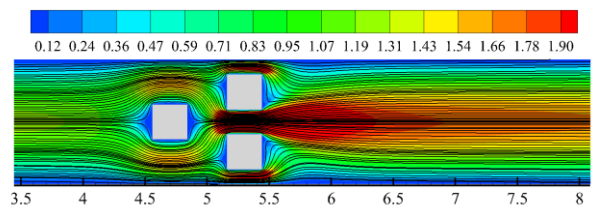
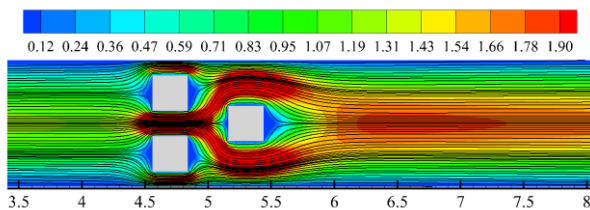
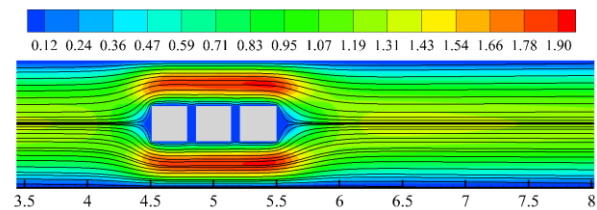
Fig. 4. Nusselt number of obstacles wall in different arrangements (1 to 5)

The non-dimensional velocity distribution through the channel as well as the streamlines are shown in Fig. 5. It can be seen that by changing the arrangement from in-line to staggered, the amount of uniform and direct velocity in X-direction decreased while the velocity in the Y-direction increased. In more detail, Figure 6 illustrates the degree of tortuosity for each arrangement. This is the relationship

between the effective length through a porous medium and the distance in a straight line between two points. In the present study it was calculated by equations 14 and 15 according to [29, 30]. As can be seen in figure 6, changing the arrangement from in-line to staggered increased the tortuosity by up to 8%.

$$\varphi = \frac{\sum_{i,j} V_{mag}(i,j)}{\sum_{i,j} |V_x(i,j)|} \quad (14)$$

$$V_{mag}(i,j) = \sqrt{V_x(i,j)^2 + V_y(i,j)^2} \quad (15)$$



3

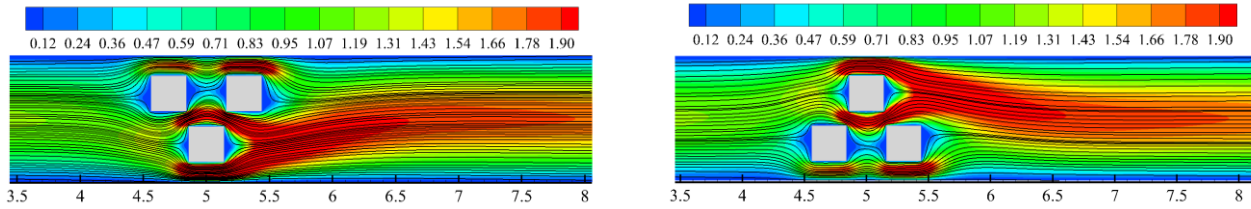


Fig. 5 – Streamlines and velocity distribution through the channel for different obstacles arrangements (1 to 5)

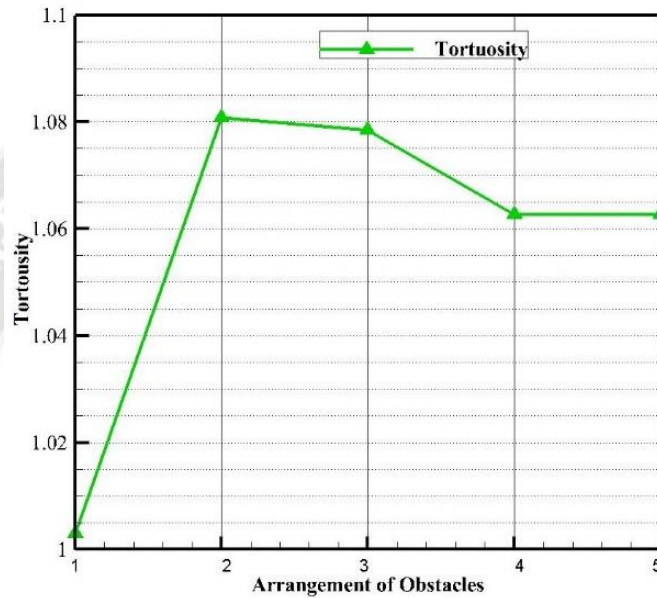


Fig. 6 –Tortuosity for different arrangements (1 to 5)

A comparison between the Nusselt number and the tortuosity of each arrangement is shown in Fig. 7. As can be seen, there is a close relationship between tortuosity and Nusselt number in these five symmetrical arrangements of tree obstacles. On

the other hand, Fig. 8 illustrates the correlation between tortuosity and Nusselt number. As can be seen, in these five symmetrical arrangements of tree obstacles, as the tortuosity increased, so did the Nusselt number.

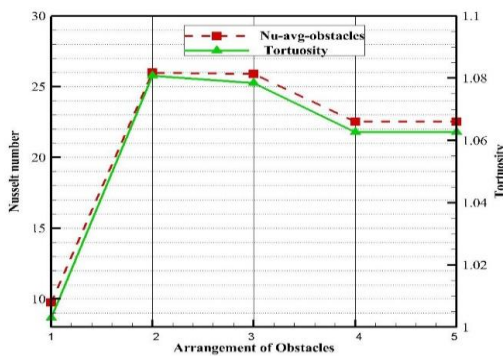


Fig. 7 – Nusselt number of the obstacles and tortuosity in different arrangements (1 to 5)

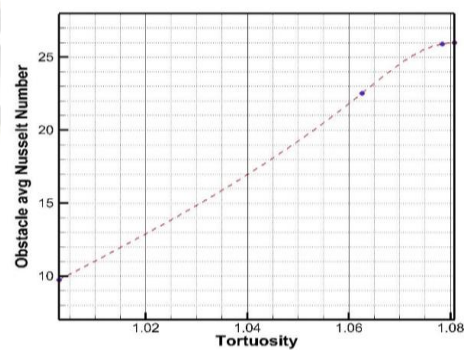


Fig. 8 – Relationship between Nusselt number of the obstacles and tortuosity in different arrangements, $\epsilon=75\%$

5 - Conclusion:

In the present study, a porous media has been simulated by Lattice Boltzmann Method and D2Q9 BGK model with the pore-scale approach. In this research, three square obstacles are represented as a solid section of a porous media. In addition, five different arrangements of obstacles including in-line and staggered are simulated. To investigate the effect of the position of obstacles in porous media of equal porosity on heat transfer and fluid flow behavior.

The results of this study showed that for the same degree of porosity ($\varepsilon=75\%$), different values of Nusselt number and tortuosity can be obtained by changing the arrangement of the obstacles. For example, the Nusselt number of the obstacles increased by up to 167% and the tortuosity increased by up to 8%. In addition, by increasing the tortuosity in these five symmetrical arrangements, the Nusselt number also increased.

References:

- [1] MORADI, Iman; D'ORAZIO, Annunziata. Lattice Boltzmann Method Pore-scale simulation of fluid flow and heat transfer in porous media: Effect of size and arrangement of obstacles into a channel. *Engineering Analysis with Boundary Elements*, 2023, 152: 83-103.
- [2] Zarei, A., Karimipour, A., Isfahani, A. H. M., & Tian, Z. (2019). Improve the performance of lattice Boltzmann method for a porous nanoscale transient flow by provide a new modified relaxation time equation. *Physica A: Statistical Mechanics and its Applications*, 535, 122453.
- [3] J. Tan, W. Keller, S. Sohrabi, J. Yang, and Y. Liu, "Characterization of nanoparticle dispersion in red blood cell suspension by the lattice boltzmann-immersed boundary method," *Nanomaterials*, vol. 6, no. 2, p. 30, 2016.
- [4] H. Shokouhmand, F. Jam, and M. Salimpour, "Simulation of laminar flow and convective heat transfer in conduits filled with porous media using Lattice Boltzmann Method," *International Communications in Heat and Mass Transfer*, vol. 36, no. 4, pp. 378-384, 2009.
- [5] M. Sheikholeslami and M. Seyednezhad, "Lattice Boltzmann method simulation for CuO-water nanofluid flow in a porous enclosure with hot obstacle," *Journal of Molecular Liquids*, vol. 243, pp. 249-256, 2017.
- [6] T. Seta, E. Takegoshi, and K. Okui, "Lattice Boltzmann simulation of natural convection in porous media," *Mathematics and Computers in Simulation*, vol. 72, no. 2-6, pp. 195-200, 2006.
- [7] H. Alihussein, M. Geier, and M. Krafczyk, "A parallel coupled lattice Boltzmann-volume of fluid framework for modeling porous media evolution," *Materials*, vol. 14, no. 10, p. 2510, 2021.
- [8] X. Ruan et al., "Strain-enhanced thermoelectric performance in GeS2 monolayer," *Materials*, vol. 15, no. 11, p. 4016, 2022.
- [9] D. S. Svyetlichnyy, "Development of the Platform for Three-Dimensional Simulation of Additive Layer Manufacturing Processes Characterized by Changes in State of Matter: Melting-Solidification," *Materials*, vol. 15, no. 3, p. 1030, 2022. [Online]. Available: <https://www.mdpi.com/1996-1944/15/3/1030>.
- [10] P. Zhao, R. Piao, and Z. Zou, "Mesoscopic Fluid-Particle Flow and Vortex Structural Transmission in a Submerged Entry Nozzle of Continuous Caster," *Materials*, vol. 15, no. 7, p. 2510, 2022.
- [11] A. M. Rausch, V. E. Küng, C. Pobel, M. Markl, and C. Körner, "Predictive Simulation of Process Windows for Powder Bed Fusion Additive Manufacturing: Influence of the Powder Bulk Density," *Materials*, vol. 10, no. 10, p. 1117, 2017. [Online]. Available: <https://www.mdpi.com/1996-1944/10/10/1117>.
- [12] M. C. Sukop and D. Or, "Lattice Boltzmann method for modeling liquid-vapor interface configurations in porous media," *Water Resources Research*, vol. 40, no. 1, 2004.
- [13] A. Leonardi, F. K. Wittel, M. Mendoza, and H. J. Herrmann, "Lattice-Boltzmann method for geophysical plastic flows," in *Recent Advances in Modeling Landslides and Debris Flows*: Springer, 2015, pp. 131-140.
- [14] R. A. Escobar, S. S. Ghai, M. S. Jhon, and C. H. Amon, "Multi-length and time scale thermal transport using the lattice Boltzmann method with application to electronics cooling," *International Journal of Heat and Mass Transfer*, vol. 49, no. 1-2, pp. 97-107, 2006.
- [15] A. D'Orazio, M. Corcione, and G. P. Celata, "Application to natural convection enclosed flows of a lattice Boltzmann BGK model coupled with a general purpose thermal boundary condition," *International Journal of Thermal Sciences*, vol. 43, no. 6, pp. 575-586, 2004.
- [16] A. D'Orazio, Z. Nikkhah, and A. Karimipour, "Simulation of copper-water nanofluid in a microchannel in slip flow regime using the lattice Boltzmann method with heat flux boundary condition," in *Journal of Physics: Conference Series*, 2015, vol. 655, no. 1: IOP Publishing, p. 012029.
- [17] J. Yang and E. S. Boek, "A comparison study of multi-component Lattice Boltzmann models for flow in porous media applications," *Computers & Mathematics with Applications*, vol. 65, no. 6, pp. 882-890, 2013.

- [18] Wang TH, Wu HC, Meng JH, Yan WM. Optimization of a double-layered microchannel heat sink with semi-porous-ribs by multi-objective genetic algorithm. *International Journal of Heat and Mass Transfer*. 2020 Mar 1;149:119217.
- [19] Hamidi E, Ganesan P, Muniandy SV, Hassan MA. Lattice Boltzmann Method simulation of flow and forced convective heat transfer on 3D micro X-ray tomography of metal foam heat sink. *International Journal of Thermal Sciences*. 2022 Feb 1;172:107240.
- [20] Wang CH, Liu ZY, Jiang ZY, Zhang XX. Numerical investigations of convection heat transfer in a thermal source-embedded porous medium via a lattice Boltzmann method. *Case Studies in Thermal Engineering*. 2022 Feb 1;30:101758.
- [21] Feng YY, Wang CH, Xiang Y, Zhang XX. Internal thermal source effects on convection heat transfer in a two-dimensional porous medium: A lattice Boltzmann study. *International Journal of Thermal Sciences*. 2022 Mar 1;173:107416.
- [22] Paknahad, R., Siavashi, M. and Hosseini, M., 2023. Pore-scale fluid flow and conjugate heat transfer study in high porosity Voronoi metal foams using multi-relaxation-time regularized lattice Boltzmann (MRT-RLB) method. *International Communications in Heat and Mass Transfer*, 141, p.106607.
- [23] S.-G. Chen, C.-H. Zhang, F. Jin, P. Cao, Q.-C. Sun, and C.-J. Zhou, "Lattice Boltzmann-discrete element modeling simulation of SCC flowing process for rock-filled concrete," *Materials*, vol. 12, no. 19, p. 3128, 2019.
- [24] D'Orazio and A. Karimipour, "A useful case study to develop lattice Boltzmann method performance: gravity effects on slip velocity and temperature profiles of an air flow inside a microchannel under a constant heat flux boundary condition," *International Journal of Heat and Mass Transfer*, vol. 136, pp. 1017-1029, 2019.
- [25] X. Huang, W. Zhou, and D. Deng, "Effective Diffusion in Fibrous Porous Media: A Comparison Study between Lattice Boltzmann and Pore Network Modeling Methods," *Materials*, vol. 14, no. 4, p. 756, 2021. [Online]. Available: <https://www.mdpi.com/1996-1944/14/4/756>.
- [26] M. Zhang, Q. Zhao, Z. Huang, L. Chen, and H. Jin, "Numerical simulation of the drag and heat-transfer characteristics around and through a porous particle based on the lattice Boltzmann method," *Particuology*, vol. 58, pp. 99-107, 2021.
- [27] Q. Liu, X.-B. Feng, and X.-L. Wang, "Multiple-relaxation-time lattice Boltzmann model for convection heat transfer in porous media under local thermal non-equilibrium condition," *Physica A: Statistical Mechanics and its Applications*, vol. 545, p. 123794, 2020.
- [28] Y.-H. Qian, D. d'Humières, and P. Lallemand, "Lattice BGK models for Navier-Stokes equation," *EPL (Europhysics Letters)*, vol. 17, no. 6, p. 479, 1992.
- [29] M. Espinoza-Andaluz, V. Velasco-Galarza, and A. Romero-Vera, "On hydraulic tortuosity variations due to morphological considerations in 2D porous media by using the Lattice Boltzmann method," *Mathematics and Computers in Simulation*, vol. 169, pp. 74-87, 2020.
- [30] Nabovati and A. Sousa, "Fluid flow simulation in random porous media at pore level using lattice Boltzmann method," in *New trends in fluid mechanics research*: Springer, 2007, pp. 518-521.